# A z-component magnetoresistive sensor

F. C. S. da Silva,[1,a] S. T. Halloran,[1] L. Yuan,[2] and D. P. Pappas[2]
[1]University of Colorado Denver, Denver, Colorado 80217-3364, USA
[2]National Institute of Standards and Technology, Boulder, Colorado 80305, USA

(Received 22 February 2008; accepted 12 March 2008; published online 8 April 2008)

A thin-film sensor bridge that measures the component of the magnetic field perpendicular to the plane of the substrate (also called the $z$-component field) is described. The sensor is fabricated on anisotropically etched, V-shaped groves on Si(100) substrates. The anisotropic magnetoresistive effect was used to measure the $z$ component of the magnetic field with a 40 dB rejection of other components. The device can be integrated with standard in-plane $x$- and $y$-component sensors to form a system with a footprint of $100 \times 100$ $\mu m^2$ and a noise floor of 20 nT at 1 Hz. © *2008 American Institute of Physics*. [DOI: 10.1063/1.2905264]

The measurement of magnetic field direction is important in applications such as compasses, geological mapping, position sensing, and searching techniques. Applications for magnetometers continue to be implemented, e.g., biomechanical monitoring of joint angle positions,[1] vehicle detection, and nondestructive testing. Magnetometers are transducers that convert magnetic field to measurable quantities such as voltages. In general, there are two categories of magnetometers: those that are sensitive to the strength and direction of the magnetic field (vectorial magnetometer) and those that are sensitive only to the strength. The latter category is useful in search coils and other detection techniques. It includes devices such as optically pumped and nuclear magnetic resonance (NMR) magnetometers that measure the magnetic field amplitude down to 70 fT (Ref. 2) with a few micrometers of spatial resolution.[3]

However, for many applications, it is critical to sense both the strength and direction of the field. Vectorial sensors in this category include Hall probes, magnetoresistive effect devices, conventional and superconducting search coils, and fluxgates. Vector magnetometers integrate multiple single-component sensors placed in three linearly independent directions. Some integrated vector magnetometer designs use micromachined electromechanical systems technology to obtain linear independence. Demonstrations of such magnetometers use Hall probes[4–6] and search coils.[7] Other designs use in-plane Hall sensors and instrumentation amplifiers to obtain all components of the magnetic field.[8] Common problems reported on such magnetometers refer to angle uncertainties, cross-talk, and nonuniform sensor response.

In this paper, we present a vector magnetometer based on anisotropic magnetoresistive (AMR) sensors[9] that mitigate these problems. Because these sensors are intrinsically sensitive to the magnetic field in the plane, it is relatively simple to fabricate a two-axis magnetometer on a flat substrate. However, combining two substrates to form a $z$ axis creates uncertainties in the angular positioning. In this paper, we focus on the $z$-component (out-of-plane) sense element and how to eliminate cross-talk and common mode fields from the $x$-$y$ (in-plane) components using a Wheatstone bridge configuration. The result is a sensor that measures the $z$ component of the magnetic field with a 100:1 rejection to other components. The system has a noise floor of 20 nT at 1 Hz and can be integrated to form a three-dimensional (3D) magnetometer.

To fabricate this sensor, we performed an anisotropic etch on the {100} surface of a Si substrate. The etchant solution contained 20% isopropyl alcohol (IPA) and 80% potassium hydroxide (KOH) at 65 °C. All percentages are in volume. The etch produced {111} planes forming a V-shaped groove (v groove) on the Si substrate. The native oxide on the Si substrate acted as a mask, and the etch depth was limited by the $x$-$y$ dimensions of the v groove and the etch duration, which was 40 min long. The addition of IPA to the solution and the relatively low etching temperature produced smooth surfaces on the etched Si without creating extra roughness on the oxide mask. After the etch, a thermal oxidation step created a 150 nm $SiO_2$ insulation layer on the v-groove surface prior to the magnetic layer deposition.

The magnetic sensor consisted of a 35 nm thick $Ni_{80}Fe_{20}$ film sandwiched by two Ta layers (3 nm in thickness each). The Ta layers helped texture (bottom) the magnetic layer and protect it against corrosion (top). This trilayer structure was deposited by magnetron sputtering at an Ar pressure of 0.27 Pa ($2 \times 10^{-3}$ Torr) after the deposition chamber reached a base pressure of $5.3 \times 10^{-6}$ Pa ($4 \times 10^{-8}$ Torr). A cylindrical permanent magnet provided a 40 kA $m^{-1}$ (500 Oe) field along the long axis of the v groove to induce a uniaxial magnetocrystalline anisotropy axis on the magnetic layer during deposition. The substrate/magnet system rotated with respect to the deposition guns to improve homogeneity and minimize glancing-angle deposition (GLAD) effects. An ion-mill step on a photoresist pattern defined the magnetic sensor geometry ($3.5 \times 20$ $\mu m^2$) in the v groove and on the substrate plane. A 200 nm Al layer, obtained by electron-beam evaporation and patterned with lift-off resist bilayers, provided the connection to single elements and four-element Wheatstone bridges.

Figure 1(a) illustrates the substrate rotation around the ⟨100⟩ axis. Because the deposition solid angle along the ⟨100⟩ axis is the same during the sample rotation, the deposition rate on the {100} plane is therefore constant. However, the solid angle for the {111} planes varies with the sample rotation. This leads to a varying deposition rate and varying deposition angle on the {111} planes. These variations are sinusoidal in time because the substrate rotates at a constant angular speed. Furthermore, because the deposition gun axis

[a]Electronic mail: fabio.dasilva@nist.gov.

 

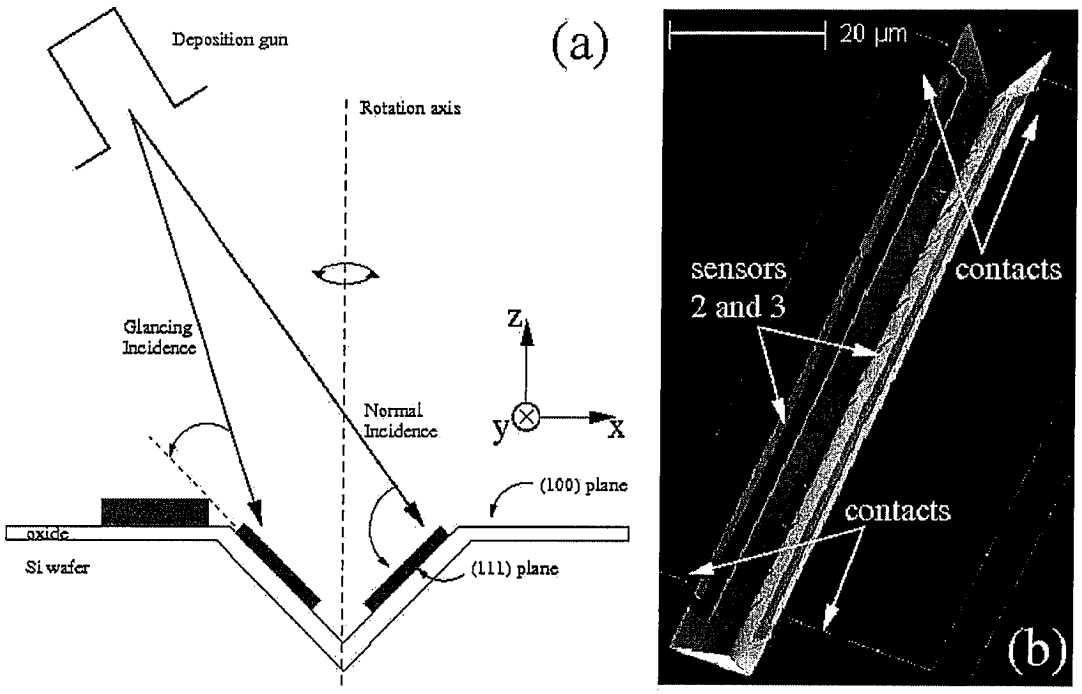


FIG. 1. (a) Deposition geometry illustrating the relative angles during deposition.(b) SEM image of two sensors defined in a micromachined v groove and their corresponding electrical contacts.

forms an angle of approximately 30° with the rotation axis, the incidence angle on the {111} planes varies from ≈90° to glancing (near 0°). In the GLAD condition, the Ta seed layer forms a columnar structure.[10] This structure reportedly induces an extra contribution to the anisotropy of thin magnetic films.[11] The induced anisotropy leads to a magnetic hardening of the sensors defined in the v groove when compared to the sensor defined on the {100} plane.

A scanning electron microscope (SEM) image of two $z$-component sensors in Fig. 1(b) shows the geometry of the sensor in the v groove and the Al contact connections. Here, the $x$ and $y$ directions coincide with the $\langle 110\rangle$ and $\langle \bar{1}10\rangle$ crystallographic axes of the substrate, respectively. Atomic force microscopy measurements of the substrate roughness in the areas exposed and not exposed to the KOH etch show an average height of 0.30 and 0.26 nm, respectively. Because of the small effect of the KOH etch on the roughness of the $SiO_2$, we expect the average roughness on the {111} planes to be in the same range as found in the {100} plane. The SEM image also shows that the lithography can connect the Al contacts to the sensors at the {100} plane. However, the actual magnetotransport measurements were performed on rectangular films connected to Al contacts in the v groove to minimize shape-induced magnetic anomalies.

Figure 2(a) shows the schematic layout of the sensors in the {100} and {111} planes. Sensor 1 senses fields along the $x$ direction. Sensors 2 and 3 sense fields in the $z-x$ plane. Figure 2(b) shows how the components of the magnetic field in the $z-x$ plane are projected along the {111} plane. The field sensed by sensors 2 and 3 in the {111} planes are $H_2=-H_a+H_b$ and $H_3=H_a+H_b$, respectively. Here, $H_a=H_z \sin\beta$ and $H_b=H_x \cos\beta$, where $\beta=54.74°$ is the angle formed by the {111} and {100} planes. We assume here that demagnetizing fields prevent the sensors from sensing fields perpendicular to their surfaces.

Magnetotransport measurements used a 10 mA current source and a voltmeter to measure the response of the sensors with respect to the applied field direction. Figure 3 shows curves of the normalized change in resistance $(R-R_0)/R_0$ versus the external field $H$ applied along the hard axis of sensors 1 and 2. Here, $R_0$ is the resistance value at

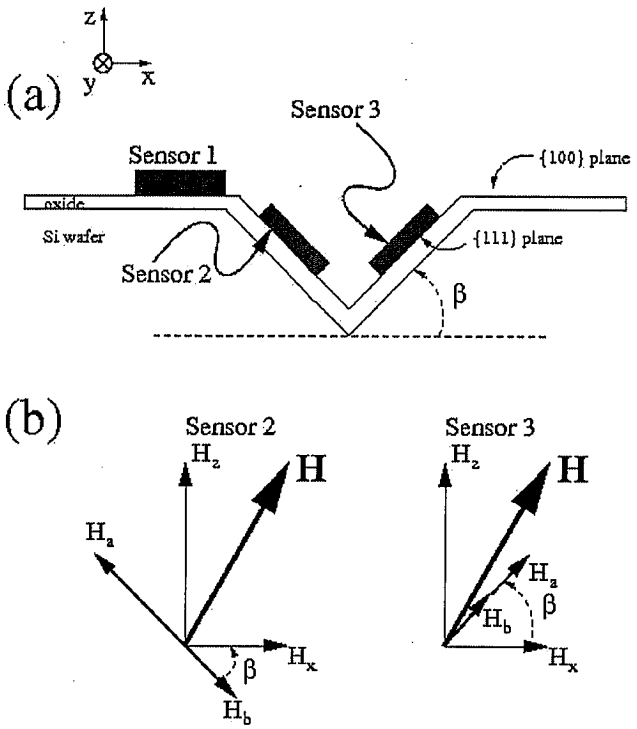


FIG. 2. (a) A schematic cross-sectional view of the sensor geometry in the $z-x$ plane. Here, $\beta=54.74°$ is the angle between the {100} and {111} planes. (b) Vector diagram of the projections of the applied field **H** in the $z-x$ plane $(H_z,H_x)$ and their respective projections on the {111} plane $(H_a,H_b)$.

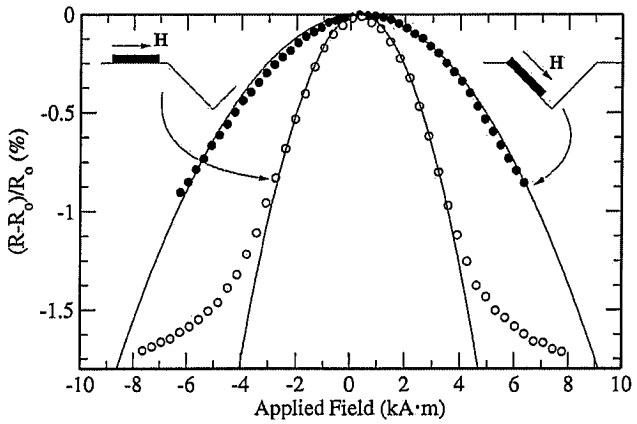


FIG. 3. Hard axis transfer curve data for sensors 1 (gray circles) and 2 (black circles). The geometry of the measurement described in the inset shows the direction of the applied field **H**. The solid lines represent a fit of the data at zero field to a parabola.

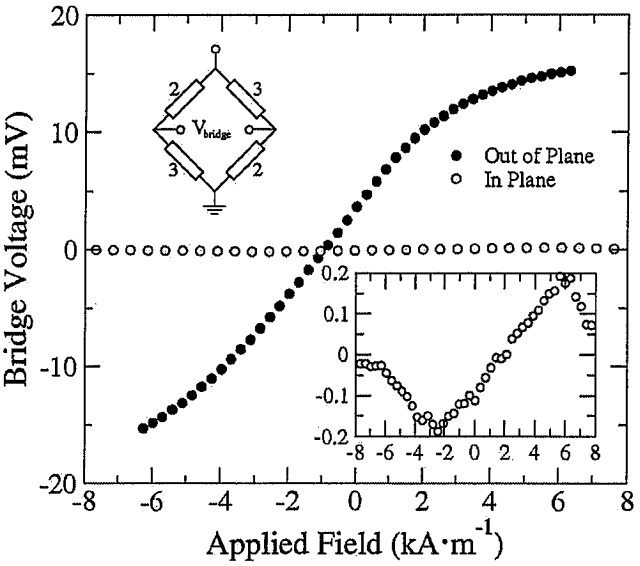


FIG. 4. Output voltage of the sensor bridge for fields in the $z$ direction (solid circles) and $x$ direction (gray circles). The upper inset shows the schematic design of the bridge where the numbers 2 and 3 correspond to sensors 2 and 3, respectively. The lower inset shows the in-plane signal magnified 100 times.

zero field, whose values are 52.6 Ω for sensor 1 and 106.5 Ω for sensor 2. The difference in $R_0$ for sensors 1 and 2 is an indication that the films deposited in the v groove are thinner by a factor of 2 than those on the {100} plane. The anisotropy field, indirectly measured here by the concavity of the parabola around zero applied field, shows an increase of 35% for sensor 2 when compared to sensor 1. This increase, attributed to the partial GLAD condition described above, overcomes the natural reduction in the anisotropy field with the thickness of the film.[12]

The difference in anisotropy fields implies a difference in sensitivity between sensors on the {100} and {111} planes. This creates problems in recovering the $z$ component of the magnetic field by using sensors 1 and 2 in a simple circuit. To solve this problem, we linearized sensors 2 and 3 to obtain the $z$ component. AMR sensors can be linearized by biasing the direction of the applied current or the direction of the magnetization vector with respect to the sensor easy axis.[13] Here, we chose to apply an external field in the $x$ direction to bias the magnetization vector of the sensors to sense $H_b - H_a$ (sensor 2) and $H_b + H_a$ (sensor 3).

Using the two sensors described above to form a Wheatstone bridge (Fig. 4), the differential voltage is then proportional to $H_z \sin \beta$. Notice here that the bridge design should be only sensitive to out-of-plane fields. The rejection of the in-plane component follows the assumption of linearized sensors and is valid for $\beta \neq 0, \pi$.

Figure 4 shows the behavior of an actual Wheatstone bridge formed by sensors in the configuration of sensors 2 and 3 in Fig. 2(a). At zero field, the sensitivity slope of the bridge to in-plane fields is 50 $\mu$V/kA m$^{-1}$ whereas for out-of-plane fields, the slope is 5 mV/kA m$^{-1}$. This corresponds to a rejection ratio for in-plane field of 100:1 or 40 dB. This result is consistent with tolerances in the lithography at the micron scales, which cause a mismatch in the sensor geometry of ≈1%.

Noise measurements helped define the sensitivity of the sensor bridge and followed the procedure described in Ref. 14. The measured noise sensitivity of the bridge at 1 Hz is 20 nT/$\sqrt{Hz}$, which makes it suitable for compass and biomechanical applications. Because the bridge has a footprint of $100 \times 100$ $\mu$m$^2$, a potential 3D magnetometer will resolve fields in space with 50 $\mu$m accuracy.

In conclusion, we have discussed the fabrication and measurement of a $z$-component magnetometer with a focus on the integration into a 3D magnetometer. A Wheatstone bridge configuration allows the system to have a 100:1 rejection of the in-plane versus out-of-plane component. The noise figure of the system and its spatial footprint make it a viable candidate for the improvement and development of current and future applications.

The authors thank Dr. Hong Wan for the insightful discussions on the subject of this paper.

[1]K. J. O'Donovan, R. Kamnik, D. T. O'Keefe, and G. M. Lyons, J. Biomech. **40**, 2604 (2007).
[2]V. Shah, S. Knappe, P. D. D. Schwindt, and J. Kitching, Nat. Photonics **1**, 649 (2007).
[3]D. Rugar, R. Budakian, H. J. Mamin, and B. W. Chui, Nature (London) **430**, 329 (2004).
[4]S. Kicin, V. Cambel, M. Kuliffayaova, D. Gregusova, E. Kovacova, and J. Novak, J. Appl. Phys. **91**, 878 (2002).
[5]D. Gregusova, V. Cambel, J. Fedor, R. Kudela, J. Soltys, and T. Lalinsky, Appl. Phys. Lett. **82**, 3704 (2003).
[6]V. Cambel, D. Gregusova, J. Fedor, R. Kudela, and S. J. Bending, J. Magn. Magn. Mater. **272-276**, 2141 (2004).
[7]J. Kyynarainen, J. Saarilahti, H. Kattelus, T. Meinander, M. Suhonen, A. Oja, H. Seppa, P. Pekko, H. Kuisma, S. Ruotsalainen, and M. Tilli, Sens. Lett. **5**, 126 (2007).
[8]C. S. Roumenin and D. I. Nikolov, Electron. Lett. **39**, 1646 (2003).
[9]A. Peczalski, J. F. Detry, H. Wan, and W. F. Witcraft, U.S. Patent No. 7,126,330 B2, (2006).
[10]M. M. Hawkeye and M. J. Brett, J. Vac. Sci. Technol. A **25**, 1317 (2007).
[11]R. D. McMichael, C. G. Lee, J. E. Bonevich, P. J. Chen, W. Miller, and W. F. Egelhoff, Jr., J. Appl. Phys. **88**, 5296 (2000).
[12]A. Aharoni, J. Appl. Phys. **83**, 3432 (1998).
[13]S. Tumanski, *Thin Film Magnetoresistive Sensors* (IOP, Bristol, 2001), p. 22.
[14]N. A. Stutzke, S. E. Russek, D. P. Pappas, and M. Tondra, J. Appl. Phys. **97**, 10Q107 (2005).